Channel estimation for massive MIMO systems based on adaptive angular domain compensation

Ting Liu
College of Information and Communication Engineering, Harbin Engineering University, Harbin, 150001, China
tingliuchn@126.com

Yong Wang
College of Information and Communication Engineering, Harbin Engineering University, Harbin, 150001, China
wangyong@hrbeu.edu.cn

Jianhong Xiang*
College of Information and Communication Engineering, Harbin Engineering University, Harbin, 150001, China
xiangjianhong@hrbeu.edu.cn

Ying Wang
College of Information and Communication Engineering, Harbin Engineering University, Harbin, 150001, China
wangyingstu@163.com

Yang Liu
Sichuan Key Laboratory of Agile Intelligent Computing, Southwest China Institute of Electronics Technology, Chengdu, 610036, China
303069077@qq.com

ABSTRACT

Millimeter-wave (mmWave) and massive Multiple Input Multiple Output (MIMO) technologies rely heavily on accurate channel state information (CSI) to significantly increase system capacity. However, the large size of the antenna array makes it more difficult to obtain accurate channel state information. We propose to utilize beam domain channels to improve the channel estimation accuracy. Specifically, we first construct the angular domain compensation. By utilizing this angular domain compensation, we further propose an angular domain compensated alternating direction multiplier method (ADC-ADMM) algorithm. The scheme models the channel estimation problem as a bi-objective convex optimization problem with joint angular domain compensation, which can capture channel state information more comprehensively. In addition, the angular domain compensation can provide a priori information and improve the robustness in noisy environments. The simulation results confirm the feasibility of the proposed ADC-ADMM scheme.

CCS CONCEPTS

• **Hardware**; • **Signal processing systems**;

KEYWORDS

Millimeter wave (mmWave), Multiple Input Multiple Output (MIMO), channel estimation, ADC-ADMM

ACM Reference Format:

Ting Liu, Yong Wang, Jianhong Xiang, Ying Wang, and Yang Liu. 2023. Channel estimation for massive MIMO systems based on adaptive angular domain compensation. In *2023 the 5th International Conference on Video, Signal and Image Processing (VSIP 2023), November 24–26, 2023, Harbin, China.* ACM, New York, NY, USA, 6 pages. https://doi.org/10.1145/3638682.3638716

*Corresponding author.

VSIP 2023, November 24–26, 2023, Harbin, China

ACM ISBN 979-8-4007-0927-2/23/11
https://doi.org/10.1145/3638682.3638716

1 INTRODUCTION

In recent years, with the rapid development of the mobile Internet and the Internet of Things (IoT), the number of smart devices accessing the network has increased dramatically. The Fifth Generation (5G) mobile communication system came into being, aiming at triggering the following significant change in the field of mobile communications [1–3]. The short wavelengths of mmWave support Massive Multiple Input Multiple Output (Massive MIMO) technology, which compensates for severe path loss, thereby improving overall network throughput and performance [4]. The base station side of a millimeter wave deployment needs to utilize accurate channel state information (CSI) to design the transmit beam. The acquisition of accurate CSI is crucial for the base station side. However, the dimension of the channel matrix in millimeter-wave scenarios increases dramatically, and it is difficult for traditional algorithms to obtain accurate CSI [5].

The mmWave channel estimation problem in [6, 7] is treated as a compressed sensing (CS) problem and the orthogonal matching pursuit (OMP) algorithm is used to recover the sparse signal. However, the limitations of the beam codebook design lead to large errors in the estimation results. Also exploiting channel sparsity for channel estimation is the vector approximate message passing (VAMP) method proposed in [8]. Literature [9] is based on the CS theory being modeled as a low-rank matrix approximation problem and solving for the channel information to be estimated via semi-positive definite programming. This method outperforms traditional least squares (LS) channel estimation schemes. However, both types of algorithms require a large number of training sequences to obtain a more satisfactory performance. The sparse mask detection (SMD) based channel estimation method in [10] reduces the dimensionality of the beamspace channel by selecting the primary beam. Then, classical algorithms such as LS are utilized to estimate the dimensionality-reduced channel. However, the SMD has a high guide frequency overhead. An alternating direction multiplier method (ADMM) based millimeter wave channel estimation scheme is proposed in [11] by combining channel sparsity and low rank. However, the lack of array gain results in poor performance at low signal-to-noise ratios (SNR).

To reduce noise interference, we propose a channel estimation scheme based on the angular domain compensation by utilizing the a priori information the channel matrix provides in the beam domain. The main contributions of the paper can be summarized as follows:

- We propose a bi-objective convex optimization problem modeling channel based on angular domain compensation. This scheme combines low rank and sparsity to capture the characteristics of the channel more comprehensively. The bi-objective convex optimization problem formulation introduces angular domain compensation, which utilizes sieveability to reject redundant signals in the channel matrix in the beam domain. The angular domain compensation helps to improve the estimation accuracy of the path direction.
- We propose a channel estimation scheme based on the angular domain compensated alternating direction multiplier method (ADC-ADMM) algorithm. When ADC-ADMM is coordinated using Lagrange multipliers, we accelerate the convergence step of ADMM by attaching a relaxation parameter to approximate the optimal solution faster.

The paper is organized as follows. Narrowband millimeter wave systems and channel models are introduced in Section 2. In Section 3, the ADC-ADMM-based channel estimation scheme is presented. To illustrate the performance of the proposed method, simulation results are shown in Section 4, and the simulation results demonstrate the effectiveness of the proposed method. The conclusion is given in Section 5.

Notation: The boldface lowercase and the boldface uppercase denote the vector and matrix, respectively. $\|\cdot\|_F$ is the Frobenius norm. $(\cdot)^T$ and $(\cdot)^H$ denote the transpose and conjugate transpose, respectively. Operands $\circ$ and $\otimes$ denote the matrix Hadamard and Kronecker products, respectively. is the expectation operator. $\mathbf{E}\{\cdot\}$ denotes the diagonal operator. $diag(\cdot)$denotes the diagonal operator. $\mathbf{I}_N$ is $N \times N$ identity matrix.

2 UPLINK IN SU-MIMO

Consider a point-to-point uplink narrowband millimeter wave system [12]. The mobile station (MS) is configured with a N_T-root antenna and the base station (BS) is configured with an N_R-root antenna. Assuming that for the first $T(0 \leq T \leq N_R N_T)$ moments of the frame, each moment sends only one unit-power lead symbol $s[t] \in \mathbb{C}(0 \leq t \leq T)$. $s[t]$ is processed by the transmitter precoding vector $\mathbf{f} \in \{0,1\}^{N_T \times 1}$ and passed through the frequency-flat channel model $\mathbf{H} \in \mathbb{C}^{N_R \times N_T}$. The BS applies the hybrid combiner $\mathbf{w} \in \{0,1\}^{N_R \times 1}$ to the received signal, then the processed received signal is $y(t) \triangleq \sqrt{P_t}\boldsymbol{w}^T \boldsymbol{H} \boldsymbol{f} s[t] + n[t]$. Where P_t is the transmitter power, $n[t]$ is the complex additive white Gaussian noise (AWGN) with zero mean and variance σ_n^2.

We consider the Saleh-Valenzuela mmWave massive MIMO channel model in [13]. The frequency domain channel $\mathbf{H}$ can be modeled as:

$$\mathbf{H} \triangleq \sum_{k=1}^{N_P} \alpha_k \mathbf{a}_R(\phi_R^{(k)}) \mathbf{a}_T^H(\theta_T^{(k)}) \tag{1}$$

where N_P the number of effective propagation paths of the channel, and $\alpha_k \in CN(0, 1/2)$ is the gain of the k-th path in the complex Gaussian distribution. $\mathbf{a}_R(\phi_R^{(k)}) \in \mathbb{C}^{N_T}$ and $\mathbf{a}_T(\theta_T^{(k)}) \in \mathbb{C}^{N_R}$ denote the array response vectors corresponding to the angle of departure (AOD) and angle of arrival (AOA) of the k-th path at the BS and MS, respectively. For the convenience of channel estimation, the frequency domain channel $\mathbf{H}$ is equivalently represented in [14] as a sparse matrix $\mathbf{S}$ containing a small number of sparse matrices with high amplitude channel gains:

$$\mathbf{H} = \mathbf{D}_R \mathbf{S} \mathbf{D}_T^H \tag{2}$$

Where $\mathbf{S} \in \mathbb{C}^{N_R \times N_T}$ is the beam domain channel. $\mathbf{D}_R \in \mathbb{C}^{N_R \times N_R}$ and $\mathbf{D}_T \in \mathbb{C}^{N_T \times N_T}$ are unitary matrices based on the normalized discrete Fourier transform (DFT) with $\mathbf{D}_R^H \mathbf{D}_R = \mathbf{I}_{N_R}$ and $\mathbf{D}_T^H \mathbf{D}_T = \mathbf{I}_{N_T}$.

3 CHANNEL ESTIMATION SCHEME

3.1 Problem formulation

Based on the matrix completeness theory with auxiliary channels [15, 16], the measurement model Eq. (1) can be re-modeled as a low-rank matrix sampling process.

$$\min_{\mathbf{H},\mathbf{S}} \tau_H \|\mathbf{H}\|_* s.t. \Omega \circ \mathbf{H} = \mathbf{H}_\Omega \tag{3}$$

Where $\tau_H > 0$ is weighting factor. $\|\mathbf{H}\|_*$ is the kernel norm of the channel matrix $\mathbf{H}$. $\Omega \in \{0,1\}^{N_R \times N_T}$ denotes the total activated antenna matrix with $M(0 \leq M \leq N_R N_T)$ non-zero terms. $\mathbf{H}_\Omega$ represents the subsampling estimation channel matrix.

The unknown CSI matrix $\mathbf{H}$ is recovered in [17] by uniting the sparse channel matrices $\mathbf{S}$. However, the spatial Fourier transform introduces a discretization error $\mathbf{E}$(let$\mathbf{Y} = \mathbf{H}$,$\mathbf{E} \triangleq \mathbf{Y} - \mathbf{D}_R \mathbf{S} \mathbf{D}_T^H$). The error accumulates in the iterations and affects the accuracy of the channel estimation. In particular, we introduce an angular domain compensation $\mathcal{P}_E$ based on the discretization error in the iterative process. The bi-objective convex optimization problem is reformulated by acting the angular domain compensation on $\mathbf{S}$:

$$\begin{aligned} &\min_{\mathbf{H},\mathbf{S}} \tau_H \|\mathbf{H}\|_* + \tau_S \|\mathcal{P}_E \circ \mathbf{S}\|_1 \\ &s.t. \mathbf{H} = \mathbf{D}_R \mathbf{S} \mathbf{D}_T^H and \Omega \circ \mathbf{H} = \mathbf{H}_\Omega \end{aligned} \tag{4}$$

Where $\tau_S > 0$ are weighting factors. The l_1-parametrization of $\mathbf{S}$ its sparsity. By acting the angular domain compensation $\mathcal{P}_E$ on $\mathbf{S}$, the redundant signals in $\mathbf{S}$ can be eliminated and the path direction estimation accuracy can be improved. The $\mathcal{P}_E^l = \Xi(\mathbf{S}^l, \delta^l)$ operation compares the elements of $\mathbf{S}^l$ and threshold δ^l. The position of an element greater than $\mathbf{E}$ is judged as a reliable path. The position of the reliable path is set adaptively based on the discretization error at each iteration, with 1 at the element corresponding to the receive or transmit angle of its reliable path, and 0 elsewhere. where l represents the number of iterations, $e_{\max}^l = \max\{e_{11}^l, \cdots, e_{ij}^l, \cdots, e_{N_R N_T}^l | e_{ij}^l \in \mathbf{E}^l\}$ denotes the largest element of $\mathbf{E}$ at l iterations. Set the threshold δ^l according to the $e_{\max}^l$

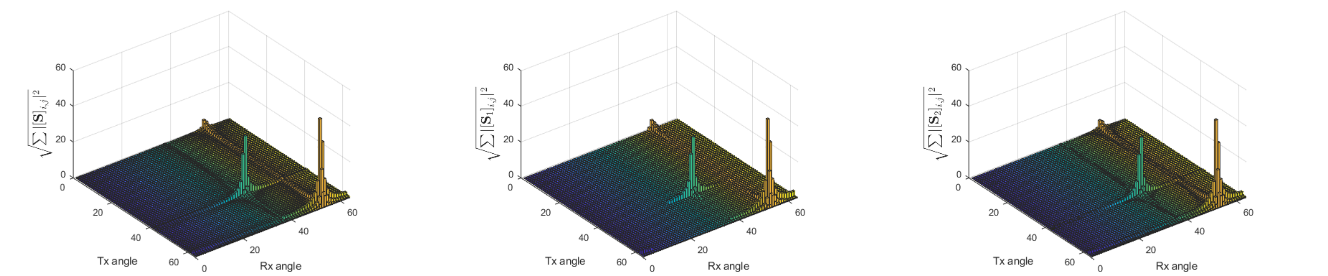

(a) Beam domain channel $\mathbf{S}$ (b) Common estimation $\mathbf{S}_1$ (c) Estimation $\mathbf{S}_2$ of the proposed program

Figure 1: Validation of the validity of the angular domain compensation. (a) represents the mean-squared coefficient magnitude in real beam domain channel, i.e., $\sqrt{\sum |[\mathrm{S}]_{i,j}|^2}$($[\mathrm{S}]_{i,j}$ denotes the (i,j)-th entry of the matrix S). (b) represents the channel estimation with common optimization problems. (c) denotes the channel estimation of the optimization problem combining the angular domain compensation.

of $\mathbf{E}^l$. It is interesting to note that the reliable path location information in $\mathcal{P}_E$ is not constant and is selected adaptively based on the discretization error within the system at each iteration. Therefore, the adaptability to different training sequences can theoretically be improved. Figure 1 verifies the effectiveness of the introduction of the angular domain compensation.

3.2 Solution scheme

We use alternating iterations to efficiently find the globally optimal solution to the optimization problem described in Eq. (4). Considering the discretization error $\mathbf{E}$ and AWGN, the augmented Lagrangian function of Eq. (4) at this point is

$$\begin{aligned}&\mathcal{L}(\mathbf{H},\mathbf{Y},\mathrm{S},\mathbf{E},\mathbf{Z}_1,\mathbf{Z}_2) \overset{\Delta}{=} \tau_H\|\mathbf{H}\|_* + \tau_S\|\mathcal{P}_E\circ\mathrm{S}\|_1\\ &+\tfrac{1}{2}\|\mathbf{E}\|_F^2 + \tfrac{1}{2}\|\Omega\circ\mathrm{Y}-\mathbf{H}_\Omega\|_F^2 + tr(\mathbf{Z}_1^H(\mathbf{H}-\mathrm{Y}))\\ &+\tfrac{\rho}{2}\|\mathbf{H}-\mathrm{Y}\|_F^2 + tr(\mathbf{Z}_2^H(\mathbf{E}-\mathrm{Y}+\mathbf{D}_R\mathrm{S}\mathbf{D}_T^H))\\ &+\tfrac{\rho}{2}\left\|\mathbf{E}-\mathrm{Y}+\mathbf{D}_R\mathrm{S}\mathbf{D}_T^H\right\|_F^2\end{aligned} \tag{5}$$

where $\mathbf{Z}_1, \mathbf{Z}_2 \in \mathbb{C}^{N_R\times N_T}$ are lag range multipliers, and ρdenotes the step size of the alternating direction method of multipliers (ADMM). According to the standard ADMM, the following separate subproblems need to be solved when the l-th$(l=0,1,\ldots)$ iteration of the algorithm is required.

The first subproblem considers the optimization of the variable $\mathbf{H}$, so only the term related to $\mathbf{H}$ in Eq. (5) is retained, which can be equivalently formulated as

$$\mathbf{H}^{l+1} = \arg\min_{\mathbf{H}} \tau_H\|\mathbf{H}\|_* + \frac{\rho}{2}\left\|\mathbf{H}-(\mathrm{Y}^{(l)}-\frac{1}{\rho}\mathbf{Z}_1^{(l)})\right\|_F^2 \tag{6}$$

According to matrix completion theory [18], Eq. (6) can be rewritten by the singular value threshold (SVT) operator as

$$\mathbf{H}^{(l+1)} = \mathbf{U}diag(\{sign(\zeta_i)\max(\zeta_i,0)\}_{1\le i\le r})\mathbf{V}^H \tag{7}$$

where $\mathbf{U}\in\mathbb{C}^{N_R\times r}$ and $\mathbf{V}\in\mathbb{C}^{N_T\times r}$ are the left and right singular vector matrices of the matrix $\mathrm{Y}^{(l)}-\frac{1}{\rho}\mathbf{Z}_1^{(l)}$, σ_i denotes the i-st of the r singular values, and $\xi_i=\sigma_i-\tau/\rho$.

The second subproblem: The derivative of Eq. (5) with respect to Yyields:

$$\frac{\partial\mathcal{L}}{\partial\mathrm{Y}} = \Omega\circ\mathrm{Y}-\mathrm{H}_\Omega-\mathrm{Z}_1^{(l)}-\rho(\mathrm{H}^{(l+1)}-\mathrm{Y})-\mathrm{Z}_2^{(l)}-\rho(\mathrm{E}^{(l)}-\mathrm{Y}+\mathrm{D}_R\mathrm{S}\mathrm{D}_T^H) \tag{8}$$

If we let Eq. (9) be zero, it is equivalent to solving the following system of equations:

$$y^{(l+1)} = (\boldsymbol{M}_1+2\rho\boldsymbol{I})^{-1}\left(\boldsymbol{h}_\Omega+\boldsymbol{z}_1^{(l)}+\rho\boldsymbol{h}^{(l+1)}+\boldsymbol{z}_2^{(l)}+\rho\boldsymbol{e}^{(l)}+\rho\boldsymbol{M}_2\boldsymbol{s}^{(l)}\right) \tag{9}$$

where$\mathbf{M}_1 \overset{\Delta}{=} \sum_{i=1}^{N_R} diag([\Omega]_i)^T\otimes\mathbf{E}_{ii}\in\mathbb{C}^{N_RN_T\times N_RN_T}$,$[\Omega]_i$ denotes the i-th row of Ω, and $\mathbf{E}_{ii}\in\mathbb{C}^{N_R\times N_R}$ denotes the insertion of a unit value in the (i,i)-th term of the all-zero matrix, $\mathbf{M}_2=\mathbf{D}_T\otimes\mathbf{D}_R$.

The third subproblem involves the solution of the angular domain compensation $\mathcal{P}_E$ and the variablesS^{l+1}. The subproblem can be equated as

$$\mathrm{S}^{l+1} = \arg\min_{\mathrm{S}} \tau_S\|\mathcal{P}_E\circ\mathrm{S}\|_1 + \frac{\rho}{2}\left\|(\frac{1}{\rho}\mathrm{Z}_2^{(l)}+\mathrm{E}^{(l)}-\mathrm{Y}^{(l+1)}+\mathrm{D}_R\mathrm{S}\mathrm{D}_T^H)\right\|_F^2 \tag{10}$$

By vectorization, such that$s^{(l+1)}=vec(\mathrm{S}^{(l+1)})$, the above equation is equivalent as

$$\mathrm{s}^{l+1} \overset{\Delta}{=} \arg\min_S \tau_S\|\mathrm{M}_3\mathrm{s}\|_1 + \frac{\rho}{2}\left\|\frac{1}{\rho}\mathrm{z}_1^{(l)}+\mathrm{e}^{(l)}-\mathrm{y}^{(l+1)}+\mathrm{D}_R\mathrm{S}\mathrm{D}_T+\mathrm{M}_2\mathrm{s}\right\|_F^2 \tag{11}$$

where$\mathbf{M}_3 \overset{\Delta}{=} \sum_{i=1}^{N_R} diag([\mathcal{P}_E]_i)^T\otimes\mathbf{E}_{ii}\in\mathbb{C}^{N_RN_T\times N_RN_T}$. Considering Eq. (11) as a standard least absolute shrinkage and selection operator (LASSO) problem [19], Eq. (10) can be equated as

$$\min_{\mathrm{S}} \tau_S\|\mathrm{M}_3\mathbf{s}\|_1 + \frac{\rho}{2}\left\|\mathrm{M}_3\mathbf{M'}_2(\frac{1}{\rho}\mathbf{z}_1^{(l)}+\mathbf{e}^{(l)}-\mathbf{y}^{(l+1)})+\mathrm{M}_3\mathbf{s}\right\|_2^2 \tag{12}$$

The soft threshold operator is then applied to the $(l+1)$iterations of Eq. (12) as follows:

$$\begin{aligned}&\boldsymbol{s}^{(l+1)} = sign\left(\mathrm{Re}(\boldsymbol{v'}^{(l+1)})\right)\circ\max(|\mathrm{Re}(\boldsymbol{v'}^{(l+1)})|-\tau'_S,0)\\ &+sign\left(Im(\boldsymbol{v'}^{(l+1)})\right)\circ\max(|Im(\boldsymbol{v'}^{(l+1)})|-\tau'_S,0)\end{aligned} \tag{13}$$

where $\mathbf{v'}^{(l+1)}=\mathrm{M}_3\mathbf{M'}_2(\frac{1}{\rho}\mathbf{z}_1^{(l)}+\mathbf{e}^{(l)}-\mathbf{y}^{(l+1)})\in\mathbb{C}^{N_TN_R\times 1}$,$\tau'_S\overset{\Delta}{=}\tau_S/\rho$.

The fourth subproblem: The derivative of Eq. (5) concerning Egives:

$$\frac{\partial \mathcal{L}}{\partial \mathbf{E}} = (1+\rho)\mathbf{E} - \rho(\mathbf{Y}^{(l+1)} - \mathbf{D}_R\mathbf{S}^{(l+1)}\mathbf{D}_T^H - \frac{1}{\rho}\mathbf{Z}_2^{(l)}) \quad (14)$$

Let Eq. (14) equal 0 to obtain the solution in closed form as follows:

$$\mathbf{E}^{(l+1)} = \frac{\rho}{\rho+1}\left\|\mathbf{Y}^{(l+1)} - \mathbf{D}_R\mathbf{S}^{(l+1)}\mathbf{D}_T^H - \frac{1}{\rho}\mathbf{Z}_2^{(l)}\right\|_F^2 \quad (15)$$

The subproblems are coordinated using Lagrange multipliers after alternately updating the variables to progressively approximate the optimal solution:

$$\mathbf{Z}_1^{l+1} = \mathbf{Z}_1^{(l)} + \beta\rho(\boldsymbol{\Omega} \circ \mathbf{Y}^{(l+1)} - \mathbf{H}_\Omega) \quad (16)$$

$$\mathbf{Z}_2^{l+1} = \mathbf{Z}_2^{(l)} + \beta\rho(\mathbf{D}_R\mathbf{S}^{(l+1)}\mathbf{D}_T^H + \mathbf{E}^{(l+1)} - \mathbf{Y}^{(l+1)}) \quad (17)$$

The introduction of relaxation parameters β in Eq. (16) and Eq. (17) and taking $\beta = 1.5$[20] increases the step size of the algorithm, leading to faster convergence, and its solution can be computed directly using Eq. (9), Eq. (13), and Eq. (15). The proposed ADC-ADMM-based channel estimation scheme is summarized in Algorithm 1. After a predetermined number of algorithm iterations $I_{\max}$, the algorithm finally outputs an estimate $\mathbf{H}^{(I_{\max})}$ of the true MIMO channel by stepwise updating and circular iterations.

Algorithm 1 Proposed ADC-ADMM-based Channel Estimation Scheme

Input: $\mathbf{H}_\Omega$, Ω, $\mathbf{D}_R$, $\mathbf{D}_T$, ρ, τ_H, τ_S, I_{max}.
Output:$\mathbf{H}^{(I_{\max})}$.
Initialization:$\mathbf{Y}^{(0)} = \mathbf{S}^{(0)} = \mathbf{E}^{(0)} = \mathbf{Z}_1^{(0)} = \mathbf{Z}_2^{(0)} = 0$.
1:**for** $l = 0, 1, \ldots, I_{\max} - 1$ **do**
2:Update $\mathbf{H}^{l+1}$ using Eq. (7),
3:Update $\mathbf{Y}^{l+1}$ using Eq. (9),
4:Update $\mathcal{P}_E = \Xi(\mathbf{S}^l, \delta^l)$,
5:Update $\mathbf{S}^{l+1}$ using Eq. (12),
6:Update $\mathbf{E}^{l+1}$ using Eq. (15),
7:Update $\mathbf{Z}_1^{l+1}$ and $\mathbf{Z}_2^{l+1}$using Eq. (16) and Eq. (17).
8:**end for**

4 SIMULATION RESULTS AND DISCUSSIONS

To verify the performance of the proposed channel estimation scheme in a mmWave massive MIMO system, the experiments were set up with a mmWave channel at 90 GHz and a system of uniform antenna linear arrays (ULAs) with $N_T \times N_R$, $N_T = 64$, and$N_R = 64$. Set the pilot symbols$[t] = 1(1 \le t \le T)$ and the transmit power $P_t = 1$ for simulation.

Considering SVT [22], OMP [6], VAMP [8], ADMM [11], ADMM-AI [21] for comparison with the proposed algorithms. Set the maximum number of iterations to $I_{\max} = 100$, and set the sparsity to N_p for OMP and VAMP. N_p denotes the number of effective propagation paths of the channel. For ADMM, ADMM-AI, and the proposed scheme, consider $\tau_H = \rho\|\mathbf{H}_\Omega\|_F$, where $\rho = 0.005$, $\tau_S = 0.1/(1 - 10\log(\sigma_n^2))$, and σ_n^2 is the noise variance. All the above tests are implemented by 100 Monte Carlo. The $NMSE$ is defined by the following equation:

$$NMSE \triangleq E\left(10\log_{10}\frac{\| \mathbf{H}^{(I_{\max})} - \mathbf{H} \|_F^2}{\| \mathbf{H} \|_F^2}\right) \quad (18)$$

where $\mathbf{H}^{(I_{\max})}$ represents the estimation of the true channel $\mathbf{H}$. The ASE is defined as follows:

$$ASE \triangleq E\left\{\log_2 \det(\mathbf{I}_{N_R} + \frac{\mathbf{H}\mathbf{H}^H}{N_T N_R(\sigma_n^2 + NMSE)})\right\} \quad (19)$$

When the parameters are configured as $N_T = 64$, $N_R = 64$, and $N_p = 2$, Figure 2 shows the $NMSE$ performance of different algorithms. The OMP is strongly influenced by the AOA discretization error. The ADMM and ADMM-AI utilize the matrix-complete theory, which is free from the beam codebook design limitation. VAMP is a statistical learning estimator that relies on training data and cannot recover the channel matrix at small T. The proposed algorithm performs well in channel estimation under the $NMSE$ metric. Therefore, an interesting conclusion is that adaptive sieving of reliable path information in the beam-domain channel matrix according to the error threshold can provide more reliable path information for channel matrix recovery.

Figure 3 shows the ASE performance of different algorithms for the parameter configurations $N_T = 64$, $N_R = 64$, and $N_p = 2$. The ASE tends to increase as the SNR increases. As shown in (19), at $T = 600$, the better the $NMSE$ performance, the higher theASE. It is interesting to note that VAMP does not show better performance than the proposed algorithm at low SNR ($SNR <$ 10**dB**) for $T = 1000$. The results show that the performance of the proposed algorithm is closest to the perfect CSI under the tested training symbols.

Figure 4 depicts the $NMSE$ performance of each algorithm versus the number of channel propagation paths N_P for $N_T = 64$, $N_R = 64$, $SNR = 30$**dB**, and $T = 1000$. As N_P increases, the $NMSE$ performance of each algorithm decreases. The $NMSE$ performance of the proposed algorithm outperforms the other algorithms in all the simulated N_P ranges. Therefore, an interesting conclusion is the adaptive sieving property of the proposed algorithm, which can adjust the threshold value according to different channel conditions, thus providing a reliable path for channel recovery.

5 CONCLUSION

In this paper, we develop a high-performance jointly optimized channel estimation scheme in narrowband mmWave Massive MIMO systems. Specifically, we first constructed the angle compensation matrix and verified the effectiveness of angular domain compensation. Based on this angular domain compensation, we then proposed an ADC-ADMM algorithm to improve the accuracy of channel estimation. Simulation results show that the proposed ADC-ADMM algorithm has the highest channel estimation accuracy compared to existing algorithms. For the future work, we will improve the complexity problem of the proposed solution scheme through low-rank optimization.

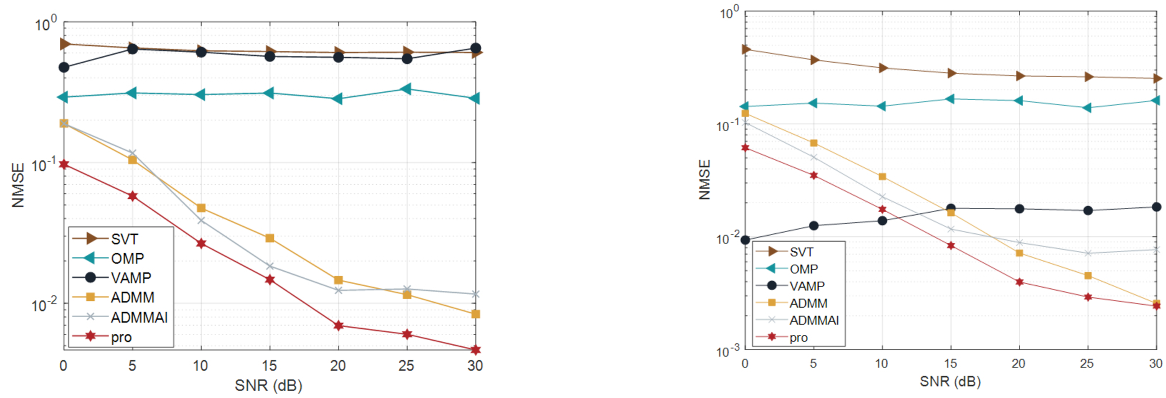

(a) T=600 (b) T=1000

Figure 2: Relationship between *NMSE* and *SNR* at different *T* values for N_T=64, N_R=64, N_P=2.

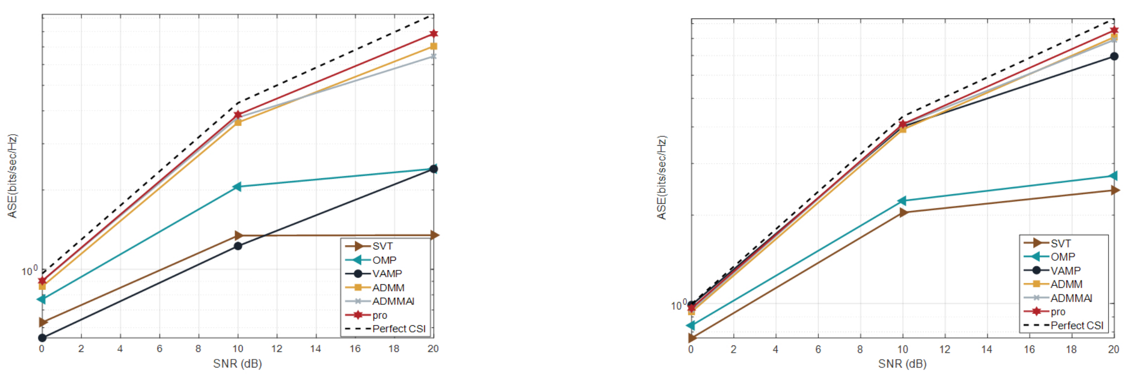

(a) T=600 (b) T=1000

Figure 3: Relationship between ASE and SNR at different T values for $N_T = 64$,$N_R = 64$,$N_p = 2$

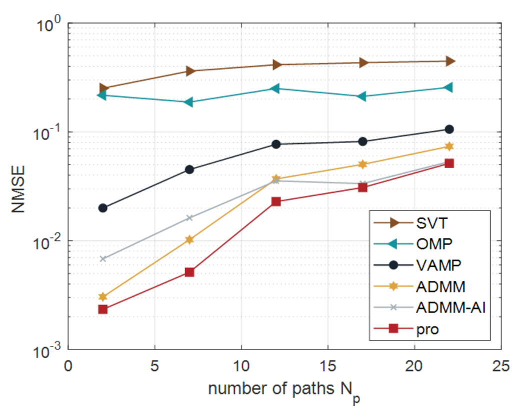

Figure 4: Relationship between $NMSE$ and N_P at different T values for $N_T = 64$,$N_R = 64$,$SNR = 30$dB,$T = 1000$

ACKNOWLEDGMENTS

This work is supported in part by Fundamental Research Funds for the Central Universities [3072022CF0801], National Key R&D Program [2018YFE0206500], National Key Laboratory of communication anti jamming technology, and Sichuan Key Laboratory of Agile Intelligent Computing. We thank all the anonymous reviewers who generously contributed their time and efforts. Their professional recommendations have greatly enhanced the quality of the manuscript.

REFERENCES

[1] Z. Xiao, L. Zhu, Y. Liu, P. Yi, R. Zhang, X.-G. Xia, and R. Schober, A Survey on Millimeter-Wave Beamforming Enabled UAV Communications and Networking. Ieee Communications Surveys and Tutorials 24 (2022) 557-610.
[2] J. Yang, J. Xu, X. Li, S. Jin, and B. Gao, Integrated communication and localization in millimeter-wave systems. Frontiers of Information Technology & Electronic Engineering 22 (2021) 457-470.
[3] Rappaport, Theodore S., *et al.* "Overview of millimeter wave communications for fifth-generation (5G) wireless networks—With a focus on propagation models." IEEE Transactions on antennas and propagation 65.12 (2017): 6213-6230.
[4] Swindlehurst, A. Lee, *et al.* "Millimeter-wave massive MIMO: The next wireless revolution?" IEEE Communications Magazine 52.9 (2014): 56-62.

[5] Fan, Jinhong, and C. Yuan. "Outage performance for two-way relaying with co-channel interference and channel estimation error." Journal of Communications 10.12(2015):963-969.

[6] R. Mendez-Rial, C. Rusu, N. Gonzalez-Prelcic, A. Alkhateeb, and R.W. Heath, Hybrid MIMO Architectures for Millimeter Wave Communications: Phase Shifters or Switches? IEEE Access 4 (2016) 247-267.

[7] Ge, Li Jun, Y. T. Cheng, and B. R. Xiao. "Joint Channel Estimation and Nonlinear Distortion Recovery Based on Compressed Sensing for OFDM Systems." Journal of Communications 11.1(2016):15-22.

[8] P. Schniter, S. Rangan, and A.K. Fletcher, Vector approximate message passing for the generalized linear model, 2016 50th Asilomar Conference on Signals, Systems and Computers, IEEE, 2016, pp. 1525-1529.

[9] S.L.H. Nguyen, and A. Ghrayeb, Compressive sensing-based channel estimation for massive multiuser MIMO systems, 2013 IEEE Wireless Communications and Networking Conference (WCNC), IEEE, 2013, pp. 2890-2895.

[10] Antón-Haro, Carles, and Xavier Mestre. "Learning and data-driven beam selection for mmWave communications: An angle of arrival-based approach." *IEEE Access* 7 (2019): 20404-20415.

[11] E. Vlachos, G.C. Alexandropoulos, and J. Thompson, Massive MIMO Channel Estimation for Millimeter Wave Systems via Matrix Completion. IEEE Signal Processing Letters 25 (2018) 1675-1679.

[12] H. Nosrati, E. Aboutanios, X. Wang, and D. Smith, Switch-based hybrid beamforming for massive MIMO communications in mmWave bands. Signal Processing 200 (2022) 108659.

[13] R.M. Larsen, Lanczos bidiagonalization with partial reorthogonalization. DAIMI Report Series (1998).

[14] J. Brady, N. Behdad, and A.M. Sayeed, Beamspace MIMO for Millimeter-Wave Communications: System Architecture, Modeling, Analysis, and Measurements. IEEE Transactions on Antennas and Propagation 61 (2013) 3814-3827.

[15] K.-Y. Chiang, C.-J. Hsieh, and I.S. Dhillon, Matrix completion with noisy side information. Advances in neural information processing systems 28 (2015).

[16] Kao, Yung-An, and KunFeng Wu. "The Research of Frequency Domain Least Squares Channel Estimation in OFDM Systems." J. Commun. 11.2 (2016): 157-163.

[17] X.J. Li, J. Fang, H.B. Li, and P. Wang, Millimeter Wave Channel Estimation via Exploiting Joint Sparse and Low-Rank Structures. Ieee Transactions on Wireless Communications 17 (2018) 1123-1133.

[18] J.-F. Cai, E.J. Candès, and Z. Shen, A singular value thresholding algorithm for matrix completion. SIAM Journal on optimization 20 (2010) 1956-1982.

[19] R. Tibshirani, Regression shrinkage and selection via the lasso. Journal of the Royal Statistical Society: Series B (Methodological) 58 (1996) 267-288.

[20] W. Liu and J. Barrett, "Numerical methods for non-linear variational problems," *ESAIM: Mathematical Modelling and Numerical Analysis,* vol. 28, pp. 725-744, 1994.

[21] E. Vlachos, G.C. Alexandropoulos, and J. Thompson, Wideband MIMO Channel Estimation for Hybrid Beamforming Millimeter Wave Systems via Random Spatial Sampling. IEEE Journal of Selected Topics in Signal Processing 13 (2019) 1136-1150.

[22] Cai, Jian-Feng, Emmanuel J. Candès, and Zuowei Shen. "A singular value thresholding algorithm for matrix completion." *SIAM Journal on optimization* 20.4 (2010): 1956-1982.